Lateral Motion of an Axially Moving Tape on a Cylindrical Guide Surface

Bart Raeymaekers[1]
e-mail: bart@talkelab.ucsd.edu

Frank E. Talke

University of California, San Diego,
Center for Magnetic Recording Research,
9500 Gilman Drive,
La Jolla, CA 92093-0401

The lateral motion of a tape moving axially over a cylindrical guide surface is investigated. The effects of lateral bending stiffness and friction force are studied and the attenuation of lateral tape motion as a function of the guide radius and friction coefficient is determined. Good agreement between numerical predictions and experimental results is observed.
[DOI: 10.1115/1.2723823]

Keywords: magnetic tape, lateral tape motion, bending stiffness, friction

1 Introduction

Lateral tape motion (LTM) is the time-dependent displacement of magnetic tape perpendicular to the tape transport direction. Lateral tape motion causes track misregistration between the read/write head and a previously written track, thereby limiting the track density that can be achieved [1]. In order to increase the track density further, the lateral displacement of tape must be decreased [2].

Several researchers have studied the dynamic behavior and vibrations of a moving web between rollers [3–11]. The effect of guides on the lateral tape motion in a tape path has been studied by only a few researchers. Ono [12] described the lateral displacement of an axially moving string on a cylindrical guide surface. Bending stiffness was not included in his model. He showed that the lateral motion was governed by a second order differential equation similar to that for one-dimensional heat flow. More recently, O'Reilly and Varadi [13] studied the dynamics of a closed loop of inextensible string which is undergoing an axial motion and of which one point is in contact with a singular supply of momentum. Taylor and Talke [14] investigated the interactions between rollers and flexible tape and showed that friction between the tape and the roller affects the lateral displacement of tape.

In this paper we have studied the lateral motion of magnetic tape as it moves over a stationary guide. We have included the effect of bending stiffness, since the area moment of the tape for the transverse direction is very large.

2 Theoretical Study

2.1 Lateral Tape Motion Including Bending Stiffness. In Figs. 1(*a*) and 1(*b*), a section of tape is shown as it moves over a cylindrical guide surface. Vector $\boldsymbol{M}$ denotes the position of a point on the centerline of the tape between boundary points s_1 and s_2 in a fixed cylindrical coordinate system $r\varphi z$ with unit vectors $\boldsymbol{e}_r, \boldsymbol{e}_\varphi, \boldsymbol{k}$.

To model the system, we make the following simplifying assumptions:

1) The magnitude of the friction force is proportional to the normal force, $F=\mu N$.
2) The lateral tape motion is sufficiently small so that only the first-order terms of the lateral displacement and the derivatives with respect to space or time must be retained.
3) Deformation of the tape is assumed small in the lateral direction (θ small). Bernoulli-Euler assumptions are employed.
4) The tape moves at a constant speed $\overline{v_0}$. Hence, $\partial\overline{v_0}/\partial s=0$.

The forces acting on a small element ds of tape are the tension force $\boldsymbol{T}$, the normal force $\boldsymbol{N}$, the friction force $\boldsymbol{F}$, and the shear force $\boldsymbol{V}$. Expressing $d\boldsymbol{T}$, $\boldsymbol{N}$, and $\boldsymbol{F}$ in r, φ, z coordinates, we obtain

$$d\boldsymbol{T}(s)=\left[-Ta\left(\frac{\partial\varphi}{\partial s}\right)^2 ds\right]\boldsymbol{e}_r+\left[\left(\frac{\partial T}{\partial s}a\frac{\partial\varphi}{\partial s}+Ta\frac{\partial^2\varphi}{\partial s^2}\right)ds\right]\boldsymbol{e}_\varphi+\left[\left(\frac{\partial T}{\partial s}\frac{\partial z}{\partial s}+T\frac{\partial^2 z}{\partial s^2}\right)ds\right]\boldsymbol{k} \tag{1}$$

$$\boldsymbol{N}=N\boldsymbol{e}_r \tag{2}$$

and

$$\boldsymbol{F}=-\frac{Na}{\overline{v_0}}\mu_\varphi\left[\frac{\partial\varphi}{\partial t}+\overline{v_0}\frac{\partial\varphi}{\partial s}\right]\boldsymbol{e}_\varphi-\frac{N}{\overline{v_0}}\mu_z\left[\frac{\partial z}{\partial t}+\overline{v_0}\frac{\partial z}{\partial s}\right]\boldsymbol{k} \tag{3}$$

where s is the spatial coordinate along the tape centerline, a is the radius of the cylindrical guide, and μ_φ and μ_z are the friction coefficient in the circumferential direction and the z direction, respectively. T is the magnitude of the tape tension vector and t represents the time. In addition, $d\boldsymbol{V}$ can be shown to be (Appendix)

$$d\boldsymbol{V}(s)=\left[2EI\frac{\partial^5 z}{\partial s^5}ds\right]\boldsymbol{e}_\varphi-\left[EI\frac{\partial\varphi}{\partial s}\frac{\partial^4 z}{\partial s^4}ds\right]\boldsymbol{e}_r-\left[EI\frac{\partial\varphi}{\partial s}a\frac{\partial^3 z}{\partial s^3}\left(\frac{\partial z}{\partial s}+\frac{\partial\varphi}{\partial s}\right)ds\right]\boldsymbol{k} \tag{4}$$

Using equilibrium of forces, we have

$$\rho w ds\frac{d^2\boldsymbol{M}}{dt^2}=d\boldsymbol{T}+\boldsymbol{F}ds+\boldsymbol{N}ds+d\boldsymbol{V} \tag{5}$$

where ρ is the tape density and w is the tape width.

Introducing (1)–(4) in (5), one can obtain equations for the $\boldsymbol{e}_r$, $\boldsymbol{e}_\varphi$, and $\boldsymbol{k}$ directions. We assume that $\overline{v_0}$ is constant. In addition, we assume that the local stress change in the tape can be neglected and that the LTM is small. Hence, we can write that

$$\frac{\partial\varphi}{\partial t}=\frac{\partial^2\varphi}{\partial t^2}=0$$

$$\frac{\partial^2(a\varphi)}{\partial s^2}=-\sin\theta\frac{\partial\theta}{ds}\ll 1$$

$$\frac{\partial z}{\partial s}=\sin\theta\ll 1$$

$$\frac{\partial(a\varphi)}{\partial s}=\cos\theta\cong 1$$

For a typical tape transport speed $\overline{v_0}=4$ m/s and tension $T=1$ N, we can neglect the inertia terms $\rho w\overline{v_0}^2$ versus the tension T for a

[1]Corresponding author.

Contributed by the Applied Mechanics Division of ASME for publication in the JOURNAL OF APPLIED MECHANICS. Manuscript received February 19, 2006; final manuscript received February 8, 2007. Review conducted by Oliver M. O'Reilly.

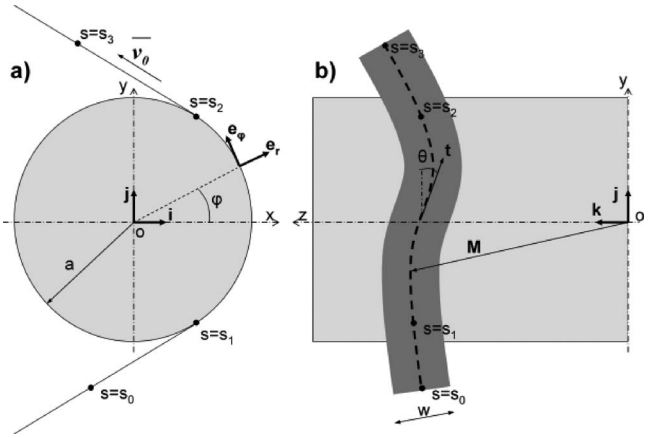

Fig. 1 Tape on a cylindrical guide

9 μm thick magnetic tape (mylar-PET) with $\rho=0.012$ kg/m^2 and $w=12.7$ mm. Hence, we obtain the equation of motion of an axially moving tape on a cylindrical guide surface as

$$-EI\frac{\partial^4 z}{\partial s^4}+T\frac{\partial^2 z}{\partial s^2}-\frac{\mu_z T}{a}(1-\nu)\frac{\partial z}{\partial s}-\frac{\mu_z T}{v_0 a}\frac{\partial z}{\partial t}=0 \tag{6}$$

$\nu=\mu_\varphi/\mu_z$ is the ratio of the friction coefficients in the circumferential and vertical direction, respectively. E represents the Young's modulus and I is the area moment. In Eq. (6), the fourth order derivative represents the bending stiffness of the tape. If the bending stiffness is neglected, i.e., $I=0$, Eq. (6) becomes identical to the equation of motion for a string derived by Ono [12].

3 Numerical Solution

To solve Eq. (6), an implicit Euler finite difference scheme was implemented. As illustrated in Figs. 1(*a*) and 1(*b*), the tape makes contact with the cylindrical guide at point s_1 and comes off the cylindrical guide at point s_2. We assume that the tape is wound on a reel with zero run-out at s_3, i.e., $z(s_3,t)=0$. At s_0, the lateral displacement $f_0(t)$ is assumed to be known from experimental measurements, i.e., $z(s_0,t)=f_0(t)$. In addition we postulate that the tape moves like a rigid body between s_0 and s_1 and s_2 and s_3, where it is not supported by the guide. The distances $l_1=|s_0s_1|$ and $l_3=|s_2s_3|$ are taken much shorter than the distance $l_2=|s_1s_2|$.

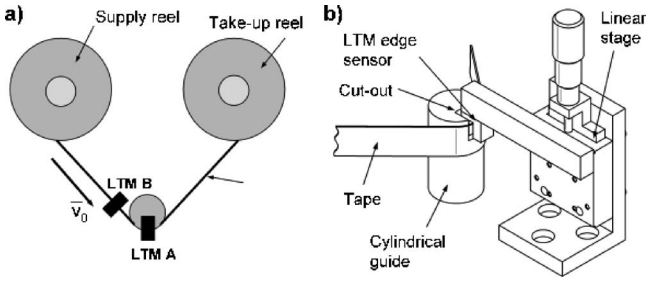

Fig. 2 Experimental apparatus to measure LTM on a cylindrical guide

The solution of Eq. (6) for the domain s_1s_2 requires four boundary conditions. The slope of the tape at $s=s_1$ must be equal to the slope at $s=s_0$ and the slope of the tape at $s=s_2$ must be equal to the slope at $s=s_3$. Thus,

$$l_1\frac{\partial z}{\partial s}-(z-f_0(t))=0 \quad \text{at } s=s_1 \tag{7}$$

and

$$l_3\frac{\partial z}{\partial s}+z=0 \quad \text{at } s=s_2 \tag{8}$$

In addition, the curvature at s_1 and s_2 has to be zero to insure a smooth tape path, i.e.,

$$\left.\frac{\partial^2 z}{\partial s^2}\right|_{s_1,s_2}=0 \tag{9}$$

4 Experimental Validation and Discussion

4.1 Apparatus. To allow a comparison of numerical results with experimental data, the apparatus shown in Fig. 2 was used. The setup consists of a tape moving from a supply reel to a take-up reel at $v_0=4$ m/s over a cylindrical guide with a radius of $a=10$ mm. The nominal tape tension $T=1$ N. The run-out of the supply reel creates LTM in the tape path. A cutout was provided in the cylinder, for the placement of a lateral tape motion edge sensor [1] (LTM A in Fig. 2(*a*)), mounted on a linear microstage for vertical positioning. Additionally, we measured the LTM as close as possible to the point where the tape makes contact with the guide (LTM B in Fig. 2(*b*)) and used this as input (boundary condition) $z(s_0,t)=f_0(t)$ for our numerical model.

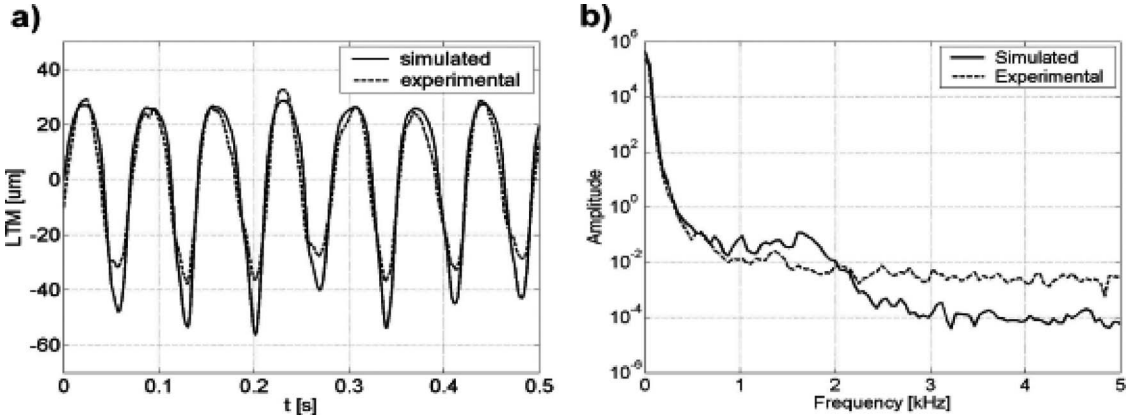

Fig. 3 Comparison of experimental measurements and numerical predictions in the middle of the cylindrical guide (*a*) in time domain and (*b*) in frequency domain

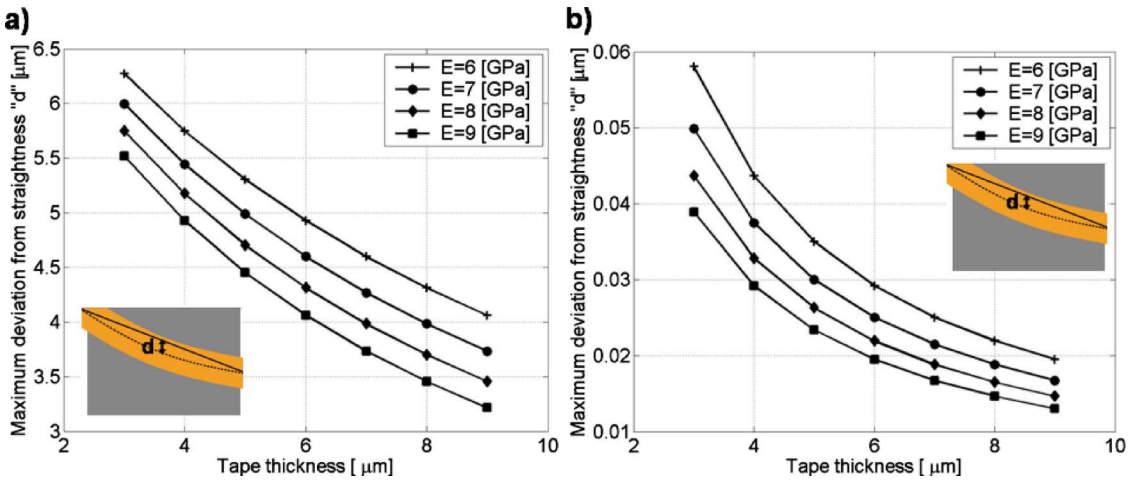

Fig. 4 Maximum deviation from straightness for (*a*) a guide with radius 100 mm and (*b*) a guide with radius 10 mm (s_0=20 μm and s_3=0 μm, $\mu_\varphi=\mu_z=0.3$)

4.2 Experimental Results. To verify our model, we have compared the values of numerically calculated lateral tape motion in the middle of the cylindrical guide with experimentally measured LTM values at the same position. Figure 3(*a*) shows simulated and experimentally measured values of lateral tape displacement in the middle of the cylindrical guide, while Fig. 3(*b*) shows the simulated and experimentally determined frequency spectrum at the same position. In our simulation we have used the following parameters: E=7 GPa, w=12.7 mm, ρ=0.012 kg/m^2, v_0=4 m/s, ρ=0.012 kg/m^2, a=10 mm, T=1 N, ν=1, and tape thickness b =9 μm. These values represent typical values for state-of-the-art magnetic tapes [15,16]. From Fig. 3 we observe good agreement between experimental measurements and numerical results, especially in the low frequency region. The increased deviation between experimental measurements and the numerical predictions for increasing frequencies is most likely related to the presence of the cutout in the stationary guide for positioning of the lateral tape displacement sensor.

4.3 Bending Stiffness. The path of a tape with bending stiffness on a cylindrical guide is different from the path followed by a string. Figure 4 shows the maximum displacement d that the tape trajectory deviates from a straight line, versus tape thickness, as a function of Young's modulus.

The results in Fig. 4(*a*) are for a cylindrical guide with a radius of 100 mm, while the results in Fig. 4(*b*) are for a cylindrical guide with a radius of 10 mm. We note that the vertical plotting scale for both pictures is different. We observe that the maximum displacement d decreases with increasing Young's modulus and increasing tape thickness, i.e., d decreases with increasing bending stiffness. In addition, the maximum deviation d decreases with decreasing guide radius.

4.4 Effect of a Guide in the Tape Path. In order to investigate the effect of a guide on the lateral tape displacement, we have calculated the amplitude ratio of the lateral tape displacement at positions s_1 and s_2. A sine wave with constant frequency was applied as an input at $s=s_1$ and the output at $s=s_2$ was simulated. For each frequency, the ratio of output to input amplitude was calculated. Figure 5(*a*) shows the amplitude ratio for a constant friction coefficient $\mu_\varphi=\mu_z$=0.3 as a function of frequency and guide radius a, while Fig. 5(*b*) shows the amplitude ratio for a guide radius of 200 mm for different friction coefficients.

We observe that the amplitude ratio decreases with increasing guide diameter and with increasing friction coefficient. By positioning guides in the tape path at specific positions, high frequency LTM could be filtered out before the tape moves over the magnetic read/write head. Lateral tape motion above 500 Hz cannot be followed by the servo system of the magnetic read/write head. When the amplitude of high frequency lateral tape motion is larger than 10% of the track width, read/write errors are likely to

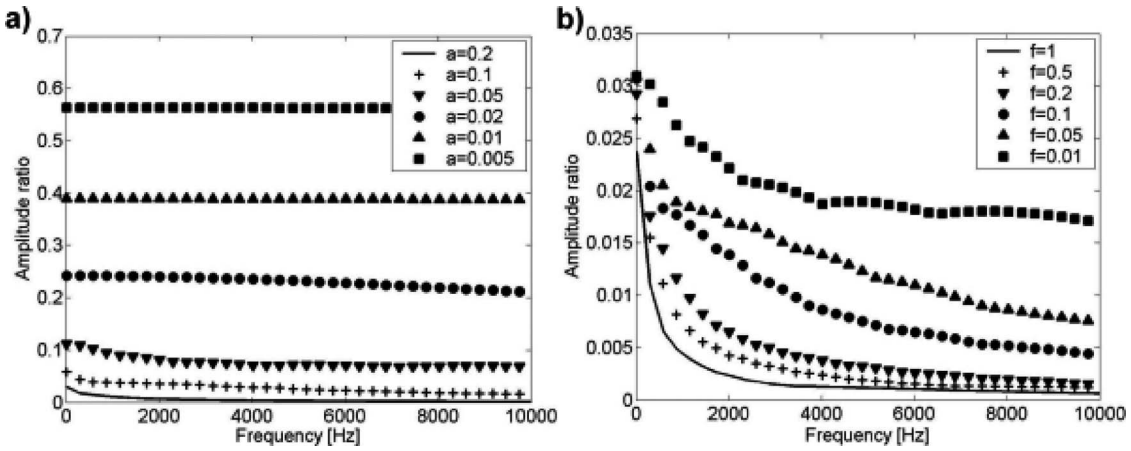

Fig. 5 Amplitude ratio $z(s_2)/z(s_1)$ (*a*) for different guide radii and (*b*) for different friction coefficients

occur. Thus, reducing high frequency lateral tape motion before it reaches the head is desirable since it would allow narrower tracks, resulting in higher track density.

The tape model with bending stiffness also has an important application in the tape slitting process where lateral tape displacement has to be minimized in order to manufacture tapes with sufficiently "straight" edges for servo track writing. If the radius of the guides that transport the tape is increased, the amplitude of the LTM is attenuated more strongly and the edge quality of the tape produced during the slitting process should be improved. Thus, optimization of the tape path by increasing the diameter of the guides should be considered in tape slitting machines to improve the quality of future tapes.

5 Conclusion

The results obtained in this paper show that:

1. Bending stiffness is an important parameter in describing the lateral displacement of a tape on a cylindrical guide surface. When modeling a tape, shear forces have to be included.
2. The effect of a cylindrical guide in the tape path can be characterized by the amplitude ratio of output and input lateral tape displacement. The amplitude ratio depends on the friction coefficient and on the contact length between tape and guide surface, i.e., the guide radius and the wrap angle. An increase in the guide radius of the tape guide or an increase in the friction coefficient between the guide surface and the tape improves the damping of both low and high LTM frequencies.
3. The bending stiffness of the tape affects its trajectory over the cylindrical guide. As the bending stiffness increases, the tape trajectory deviates less from a straight line.

Appendix

The shear force vector $\boldsymbol{V}$ with respect to the r,φ,z coordinate system can be written as

$$\boldsymbol{V} = V\boldsymbol{v} = V\frac{\partial z}{\partial s}\boldsymbol{e}_\varphi - V\frac{a\,\partial\varphi}{\partial s}\boldsymbol{k} \tag{A1}$$

The unit shear vector $\boldsymbol{v}$ can be written as

$$\boldsymbol{v} = \frac{\partial z}{\partial s}\boldsymbol{e}_\varphi - \frac{a\,\partial\varphi}{\partial s}\boldsymbol{k} \tag{A2}$$

thus,

$$\frac{\partial \boldsymbol{v}}{\partial s} = \frac{\partial^2 z}{\partial s^2}\boldsymbol{e}_\varphi - \frac{\partial z}{\partial s}\frac{\partial\varphi}{\partial s}\boldsymbol{e}_r - \frac{a\partial^2\varphi}{\partial s^2}\boldsymbol{k} \tag{A3}$$

Combining (A1)–(A3) with $d\boldsymbol{V}(s)=\boldsymbol{v}\frac{\partial V}{\partial s}ds+V\frac{\partial \boldsymbol{v}}{\partial s}ds$, $V=\frac{\partial C}{\partial s}$, and $C=EI\frac{\partial^2 z}{\partial s^2}$, yields Eq. (4).

References

[1] Taylor, R. J., Strahle, P., Stahl, J., and Talke, F. E., 2000, "Measurement of Cross-Track Motion of Magnetic Tapes," J. Inf. Storage Process. Syst., **2**, pp. 255–261.

[2] Richards, D. B., and Sharrock, M. P., 1998, "Key Issues in the Design of Magnetic Tape for Linear Systems of High Track Density," IEEE Trans. Magn., **34**(4), pp. 1878–1882.

[3] Norwood, R. E., 1969, "Effects of Bending Stiffness in Magnetic Tape," IBM J. Res. Dev., **13**(2), pp. 205–208.

[4] Shelton, J. J., and Reid, K. N., 1971, "Lateral Dynamics of an Idealized Moving Web," ASME J. Dyn. Syst., Meas., Control, **93**, pp. 187–192.

[5] Shelton, J. J., and Reid, K. N., 1971, "Lateral Dynamics of a Real Moving Web," ASME J. Dyn. Syst., Meas., Control, **93**, pp. 180–186.

[6] Wickert, J. A., and Mote, Jr., C. D., 1990, "Classical Vibration Analysis of Axially Moving Continua," ASME J. Appl. Mech., **57**, pp. 738–744.

[7] Young, G. E., and Reid, K. N., 1993, "Lateral and Longitudinal Dynamic Behavior and Control of Moving Webs," ASME J. Dyn. Syst., Meas., Control, **115**, pp. 309–317.

[8] Lee, S., and Mote, Jr., C. D., 1999, "Wave Characteristics and Vibration Control of Translating Beams by Optimal Boundary Damping," ASME J. Appl. Mech., **121**, pp. 18–25.

[9] Garziera, R., and Amabili, M., 2000, "Damping Effect of Winding on the Lateral Vibration of Axially Moving Tapes," ASME J. Vibr. Acoust., **122**, pp. 49–53.

[10] Benson, R. C., 2002, "Lateral Dynamics of a Moving Web With Geometrical Imperfection," ASME J. Dyn. Syst., Meas., Control, **124**, pp. 25–34.

[11] Yerashunas, J. B., De Abreu-Garcia, J. A., and Hartley, T. T., 2003, "Control of Lateral Motion in Moving Webs," IEEE Trans. Control Syst. Technol., **11**, pp. 684–693.

[12] Ono, K., 1979, "Lateral Motion of an Axially Moving String on a Cylindrical Guide Surface," ASME J. Appl. Mech., **46**, pp. 905–912.

[13] O'Reilly, O. M., and Varadi, P. C., 2004, "On Some Peculiar Aspects of Axial Motions of Closed Loops of String in the Presence of a Singular Supply of Momentum," ASME J. Appl. Mech., **71**, pp. 541–545.

[14] Taylor, R. J., and Talke, F. E., 2005, "Investigation of Roller Interactions With Flexible Tape Medium," Tribol. Int., **38**, pp. 599–605.

[15] Berry, B. S., and Pritchet, W. C., 1988, "Elastic and Viscoelastic Behaviour of a Magnetic Recording Tape," IBM J. Res. Dev., **32**(5), pp. 682–694.

[16] Bhushan, B., and Tao, Z., 2004, "Mechanical, Hygroscopic, and Thermal Properties of Metal Particle and Metal Evaporated Tapes and Their Individual Layers," J. Appl. Polym. Sci., **92**, pp. 1319–1345.